Toward the production of quantum degenerate bosonic polar molecules, $^{41}K^{87}Rb$

To cite this article: K Aikawa *et al* 2009 *New J. Phys.* **11** 055035

View the article online for updates and enhancements.

Toward the production of quantum degenerate bosonic polar molecules, ^{41}K^{87}Rb

K Aikawa[1], D Akamatsu[2], J Kobayashi[2], M Ueda[3,4], T Kishimoto[5] and S Inouye[2,4,6]

[1] Department of Applied Physics, University of Tokyo, Bunkyo-ku, Tokyo 113-8656, Japan

[2] Institute of Engineering Innovation, University of Tokyo, Bunkyo-ku, Tokyo 113-8656, Japan

[3] Department of Physics, University of Tokyo, Hongo, Bunkyo-ku, Tokyo 113-0033, Japan

[4] ERATO Macroscopic Quantum Control Project, JST, Bunkyo-ku, Tokyo 113-8656, Japan

[5] University of Electro-Communications, 1-5-1 Chofugaoka, Chofu 182-8585, Japan

E-mail: inouye@sogo.t.u-tokyo.ac.jp

Abstract. We review our experimental progress toward achieving the production of quantum degenerate bosonic polar molecules, ^{41}K^{87}Rb. Our primary goal is to transfer quantum degenerate Feshbach molecules into the absolute ground state via the stimulated Raman adiabatic passage (STIRAP). We have achieved a dual-species Bose–Einstein condensate of ^{41}K and ^{87}Rb in a magnetic trap, which consists of $N_{\mathrm{K}} = 1.4 \times 10^4$ potassium atoms and $N_{\mathrm{Rb}} = 3.5 \times 10^4$ rubidium atoms. An optimum optical transition for STIRAP is being identified by a separate experiment based on photoassociation in a dual-species magneto-optical trap of ^{41}K and ^{87}Rb.

[6] Author to whom any correspondence should be addressed.

IOP Institute of Physics ⏀ DEUTSCHE PHYSIKALISCHE GESELLSCHAFT

Contents

1. Introduction

Quantum degenerate gases of polar molecules are regarded as one of the most exotic quantum many-body systems for the anisotropic and long-range nature of dipole–dipole interaction. Novel quantum phases, such as crystal [1] and supersolid [2], are predicted for a Bose–Einstein condensate of polar molecules. The dipole–dipole interaction between molecules in an optical lattice is expected to pave the way for simulating a spin system [3], while the controllability of the anisotropic interaction via a microwave [4] will offer a new tool to explore the physics of a quantum many-body system.

To achieve quantum degenerate polar molecules, many approaches have been devised and implemented [5]. Recently, significant advance has been made in the 'indirect approach', which is based on associating ultracold atoms to form ultracold diatomic polar molecules. Here the process involves two steps: the first is to form loosely bound molecules by photoassociation or magneto-association at a Feshbach resonance of ultracold atoms and the second is to transfer them to their lowest rovibrational level via optical transitions such as stimulated emission pumping (SEP) or stimulated Raman adiabatic passage (STIRAP) [6]. The second process is required to cope with the following two unfavorable characteristics of loosely bound molecules: firstly, loosely bound molecules are unstable against collisions (vibrational quenching), and secondly, they have a negligible dipole moment since atoms in the molecule are well separated. Thus, transferring loosely bound molecules to the absolute ground state is very important.

This two-step scheme was originally demonstrated at Yale for laser-cooled ^{85}Rb and ^{133}Cs atoms to form ultracold ^{85}Rb^{133}Cs molecules in their absolute ground state [7]. In that pioneering work, a combination of photoassociation and SEP was employed. However, a further quest for atomic cooling and improvement in the transfer efficiency is needed for realizing quantum degeneracy with polar molecules.

Here we employ an alternative strategy that combines magneto-association at a Feshbach resonance and STIRAP. Magneto-association can transfer atoms to a single molecular level at nearly 100% efficiency. STIRAP realizes a conversion efficiency of 100% since it uses a two-photon dark state where population between two molecular states can be controlled by the

relative intensity of two lasers. Moreover, there are no heating processes in these steps. Thus, this combination should enable us to convert quantum degenerate atoms to quantum degenerate polar molecules. Intensive efforts to obtain quantum degenerate molecules in this scheme have been made for bosonic Rb_2 [8] and Cs_2 [9] molecules at Innsbruck and for fermionic $^{40}K^{87}Rb$ molecules at JILA [10].

We are aiming at achieving a Bose–Einstein condensate of polar molecules. To produce bosonic polar molecules from atoms, there are two possible choices for constituent atoms, i.e. two fermionic species or two bosonic species. Choosing two fermionic species for constituent atoms has an advantage in that Feshbach molecules are expected to have a long lifetime due to the Pauli exclusion principle. There are not many combinations of atomic species left for this approach because (a) it is natural to choose an alkali–alkali combination to make use of a magnetically tuned Feshbach resonance and (b) known stable fermionic alkali species are only ^6Li and ^{40}K. The possibility of performing efficient STIRAP for LiK is yet to be explored, since knowledge about the molecular potentials of LiK is currently limited. An experiment in this approach is ongoing in Munich [11].

In contrast, there are several possible combinations for choosing two bosonic species. Molecular potentials of both ground states and excited states are already well known for some of the combinations. Among others, $^{41}K^{87}Rb$ has the advantage that Feshbach resonances have been reported at low magnetic fields [12] and all the associated scattering lengths (a_{Rb}, a_K and a_{KRb}) are positive [13]. In addition, a high photoassociation rate of KRb [14] enables us to explore molecular potentials using photoassociated molecules. A drawback of using two bosonic species is that Feshbach molecules tend to have a short lifetime because there is no suppression of collisions [15]. This problem can be circumvented by putting atoms in an optical lattice before applying magneto-association [16]. We note that a combination of ^{87}Rb and ^{133}Cs is yet another attractive possibility since molecular potentials in the excited states have been investigated in detail [17] and many Feshbach resonances have been reported [18].

Here we report our progress toward achieving a quantum degenerate gas of $^{41}K^{87}Rb$ molecules based on magneto-association and STIRAP. Our efforts involve the production of a mixture of ^{41}K and ^{87}Rb Bose–Einstein condensates and the search for an optimum intermediate state for STIRAP via spectroscopy of $^{41}K^{87}Rb$ molecules.

In the following, section 2 discusses important parameters that set the ultimate efficiency for magneto-association and STIRAP. Section 3 describes our experimental set-up to obtain a double-species Bose–Einstein condensate of ^{41}K and ^{87}Rb. Section 4 presents our spectroscopic studies on photoassociated KRb molecules. Section 5 summarizes the obtained results and discusses future prospects.

2. Key issues in the experimental design

STIRAP is expected to acheive 100% transfer efficiency when the whole population is held in a dark state. However, the efficiency is decreased when the dark state is perturbed. The efficiency of a STIRAP transfer at a two-photon resonance is given by [19]

$$P = \exp\left(-\frac{\pi^2 \Gamma}{\Omega_0^2 \tau} - \frac{D\tau}{2}\right),\tag{1}$$

where Γ is the natural linewidth of the excited state, τ is the pulse duration, D is the linewidth associated with the frequency difference between the two lasers and Ω_0 is the reduced

Rabi frequency, which is defined as $\Omega_0 = \sqrt{\Omega_P^2 + \Omega_S^2}$, where $\Omega_P(\Omega_S)$ is the peak Rabi frequency of the pump (Stokes) field[7]. Here the first term describes the reduction of efficiency due to diabatic processes, while the second term describes the limitation due to decoherence. From equation (1), we can derive the necessary condition for an efficient transfer:

$$\frac{\Omega_0^2}{\pi^2 \Gamma} \gg \frac{1}{\tau} \gg D. \qquad (2)$$

Thus, reducing the linewidth D helps reduce the intensity required for a successful transfer.

The Rabi frequency in equation (2) depends on the Franck–Condon factor, which is a measure of the wavefunction overlap between the ground and excited states:

$$\Omega_{P(S)}^2 = d^2 E_{P(S)}^2 |\langle e|g_{P(S)}\rangle|^2. \qquad (3)$$

Here d is a transition dipole moment, $E_{P(S)}$ is an electric field of the pump (Stokes) laser and $|\langle e|g_{P(S)}\rangle|^2$ is a Franck–Condon factor between an excited state and a loosely bound level (the lowest rovibrational level). We assume that the transition dipole moment does not depend on the internuclear distance. To achieve a high transfer efficiency, one must identify a transition with a large Franck–Condon factor. Thus, it becomes imperative to perform a molecular spectroscopy to find the details of interatomic potential.

Now let us examine if one can satisfy condition (2) in the actual experiment using the parameters for ^{41}K^{87}Rb. The differential frequency of two independent lasers can be stabilized to within $D \sim 2\pi \times 10$ kHz by locking them to a stable high-finesse cavity. To satisfy the condition of D and τ in (2), the pulse duration should be $\tau \sim 1\,\mu$s. The time variation of laser intensity of the order of $1\,\mu$s is easily achieved by an acousto-optical modulator. The condition of Ω_0, Γ and τ in (2) then gives a limitation on the Rabi frequency:

$$\frac{\Omega_0^2}{\Gamma} \gg 10^7\,\text{s}^{-1}. \qquad (4)$$

For the KRb molecule, the $(3)^1\Sigma^+$ is a good candidate for the intermediate state as explained in section 4. This state has a transition dipole moment of $\sim 1ea_0$ [20], which corresponds to a natural linewidth of $\sim 2\pi \times 500$ kHz. The Franck–Condon factors between this state and the ground state are of the order of 10^{-2} [21]. Substituting these values into the inequality (4), we obtain a required Rabi frequency $\Omega_0 \sim 2\pi \times 3$ MHz and a required intensity $I \sim 600$ mW cm^{-2}. Since the typical size of a Bose–Einstein condensate is less than $100\,\mu$m, the power necessary for an efficient transfer is less than $100\,\mu$W, which is easily obtained by using a semiconductor laser.

Another key issue that affects the efficiency of STIRAP is the closed-channel fraction of Feshbach molecules, which contributes dominantly to the Franck–Condon factor. In general, the closed-channel fraction of Feshbach molecules away from the resonance is larger than that close to the resonance. However, the absolute amount of the closed-channel fraction depends strongly on the width (or the coupling strength) of the resonance [22]: molecules formed at a broad resonance are strongly perturbed by an atomic channel even away from the resonance, while those formed at a narrow resonance are dominated by the closed channel except very near the resonance. Thus, it is beneficial for us to use a narrow Feshbach resonance for the preparation of molecules with a large Franck–Condon factor. However, there is a drawback in

---

[7] In this expression, $\Omega_P \simeq \Omega_S$ is assumed.

IOP Institute of Physics Φ DEUTSCHE PHYSIKALISCHE GESELLSCHAFT

using closed-channel-dominated molecules: they can easily decay via vibrational quenching due to a large wavefunction overlap with low-lying molecular levels. To avoid this problem, atoms should be loaded into an optical lattice before they are converted to molecules.

To date, two Feshbach resonances have been reported for ^{41}K^{87}Rb at 35 G with a width of 37 G and at 79 G with a width of 1.2 G [12, 13]. Apparently, the former is a broad resonance, while the latter is a narrow resonance. In fact, coupled channel calculations indicate that a closed-channel fraction of Feshbach molecules formed at the 79 G resonance exceeds 90% below 70 G [21]. Based on the above discussions, we conclude that the resonance at 79 G is appropriate for the preparation of molecules with a large closed-channel fraction.

3. Double-species Bose–Einstein condensate of ^{41}K and ^{87}Rb

3.1. Experimental set-up

Our experimental apparatus for the production of a Bose–Einstein condensate of ^{41}K and ^{87}Rb is based on a double MOT system. Two-stage differential pumping was employed to realize a high vapor pressure ($\sim 10^{-8}$ Torr) for both potassium and rubidium and an ultra-high vacuum of 3×10^{-11} Torr. The first cell contained home-made enriched ^{41}K dispensers and commercial Rb dispensers. The cell was kept at 50 °C in order to increase the loading efficiency of potassium. For evaporative cooling of both potassium and rubidium atoms, the cloverleaf trap with a magnetic field gradient of 292 G cm^{-1} and a curvature of 67 G cm^{-2} was constructed around the second cell. Typically, 10^9 ^{41}K atoms and 10^9 ^{87}Rb atoms were simultaneously collected in a MOT in the first cell and continuously pushed to the second cell by resonant laser beams. The pushing laser for potassium was resonant with the $F = 1$ to $F' = 2$ transition, while that for rubidium was resonant with the $F = 2$ to $F' = 3$ transition. The pushed atoms had a velocity of around 20 m s^{-1} and were captured again by the MOT in the second cell. The loading efficiency of the second MOT depends on the diameter and intensity of both cooling and repumping beams of the second MOT. For potassium, a loading rate of 3×10^8 atoms s^{-1} was obtained at an e^{-2} beam diameter of about 20 mm and a total intensity of about 50 mW cm^{-2}.

3.2. Production of a ^{41}K Bose–Einstein condensate

Bose–Einstein condensation of ^{41}K atoms was first realized by sympathetic cooling with rubidium atoms [23]. After that, we reported the successful production of a Bose–Einstein condensate of ^{41}K with a large number of atoms by means of direct evaporative cooling [24]. Here, we briefly describe two key issues for achieving a Bose–Einstein condensate of ^{41}K without sympathetic cooling.

The first issue is the complexity in laser cooling of ^{41}K. It originates from the fact that the hyperfine splitting between $F' = 3$ and $F' = 2$ in the 4^3P$_{3/2}$ state is as small as 13.6 MHz. This is of the same order as the natural linewidth of this excited state (6.2 MHz). Thus, it is practically impossible to form a closed transition for laser cooling since off-resonance excitations to nearby levels such as $F' = 2$ and $F' = 1$ are not negligible. To cope with this problem, we have prepared almost the same amount of laser power for both cooling and repumping beams and detuned both lights below the whole hyperfine manifold by about 20 MHz [25]. Although this configuration enabled us to trap a large number of atoms, it led to a high temperature of about 5 mK and a low density of about 1×10^{10} cm^{-3}. The obtained phase-space density at this stage was about 10^{-9}.
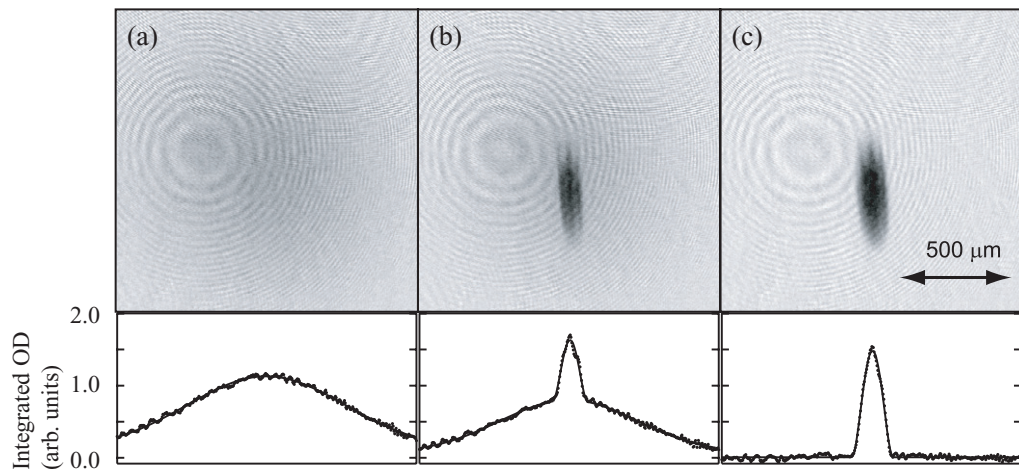
Figure 1. Realization of Bose–Einstein condensation of ^{41}K atoms by direct evaporation in a magnetic trap [24]. Absorption images of ^{41}K atoms after 40 ms expansion show (a) a thermal cloud at $T = 750$ nK, (b) a bimodal distribution at $T = 580$ nK and (c) an almost pure condensate of 3×10^5 atoms. The evaporative cooling was performed by driving rf-transition between hyperfine levels of ^{41}K atoms. No coolant was involved in the experiment.

By introducing additional stages for spatial compression and Doppler cooling [26], we were able to reach a phase-space density of 10^{-6}, which was a good starting point for evaporative cooling.

The second key issue is the necessity of using the hyperfine transition for evaporative cooling. We could not obtain a Bose–Einstein condensate of ^{41}K atoms by driving transitions between Zeeman sublevels. This was presumably because the rate constants of inelastic processes involving atoms in the $F = 2, m_F = 1$ state [27, 28] were higher for ^{41}K than for ^{87}Rb. We confined atoms in the $F = 2, m_F = 2$ state in a magnetic trap and performed evaporative cooling by driving the hyperfine transition to the $F = 1, m_F = 1$ state. Typical frequencies needed for evaporation were less than 400 MHz, since the hyperfine splitting of ^{41}K atoms in the ground state is only 254 MHz. By evaporating atoms in the $F = 2, m_F = 2$ state while constantly removing atoms in the $F = 2, m_F = 1$ state, it was possible to achieve Bose–Einstein condensation as shown in figure 1 [24]. The typical number of atoms in a pure condensate was 3×10^5.

3.3. Quantum degenerate mixture of ^{41}K and ^{87}Rb

We have also succeeded in producing a quantum degenerate mixture of ^{41}K and ^{87}Rb in a magnetic trap. We first loaded almost the same number of ^{41}K and ^{87}Rb atoms into a magnetic trap and performed evaporative cooling of both ^{41}K and ^{87}Rb atoms by driving the $F = 2, m_F = 2$ to $F = 1, m_F = 1$ transition simultaneously. However, we observed significant losses of atoms for both species. Thus, we switched to sympathetic cooling of ^{41}K by ^{87}Rb [23]. So far, we have succeeded in achieving a dual-species Bose–Einstein condensate with up to 1.4×10^4 atoms for ^{41}K and 3.5×10^4 atoms for ^{87}Rb (figure 2).
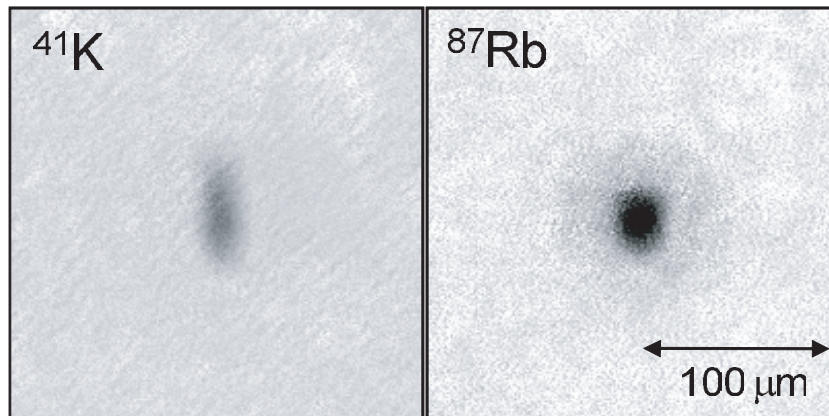
Figure 2. Images of dual Bose–Einstein condensates of ^{41}K and ^{87}Rb atoms after 20 ms of expansion. The evaporative cooling was performed by driving the $F = 2, m_F = 2$ to $F = 1, m_F = 1$ transition for the ^{87}Rb atom. ^{41}K atoms were sympathetically cooled as in [23]. The numbers of atoms in these images were 3.5×10^4 and 1.4×10^4 for Rb and K atoms, respectively.

4. Spectroscopy toward STIRAP

4.1. Selecting the optimum path for STIRAP

The optimum state for STIRAP should have large Franck–Condon factors with both weakly bound levels and the lowest rovibrational level. To understand which state can be used as an intermediate state, knowledge of the excited states of molecules is required. Here we briefly explain the excited states of alkali diatomic molecules with electronic orbital angular momentum L of 1. There are extensive spectroscopic data for these states that facilitate our spectroscopy. Since an alkali dimer has a total spin $S = 0$ (singlet) or $S = 1$ (triplet), there are four excited states labeled as $^1\Sigma^+$, $^1\Pi$, $^3\Sigma^+$ and $^3\Pi$ in Hund's case (a). Figure 3 shows the calculated potential energy curves of the ground and excited states of KRb molecule in Hund's case (a) [29]. In Hund's case (c), these states are coupled by the spin–orbit interaction to yield four components: $\Omega = 0^+$ ($^1\Sigma^+$ and $^3\Pi$), 0^- ($^3\Sigma^+$ and $^3\Pi$), 1 ($^1\Pi$, $^3\Sigma^+$ and $^3\Pi$) and 2 ($^3\Pi$), where Ω is a projection of total angular momentum $\vec{J} = \vec{L} + \vec{S}$.

The Franck–Condon factor depends not only on the spatial overlap but also on the spin component of the wavefunction. Since a Feshbach molecule has both spin triplet and singlet components, there are two possible paths to transfer it to the absolute ground state: (a) Feshbach molecule (triplet component) $\rightarrow$ intermediate state (spin mixed) $\rightarrow$ the absolute ground state (singlet) or (b) Feshbach molecule (singlet component) $\rightarrow$ intermediate state (singlet) $\rightarrow$ the absolute ground state (singlet).

The first scheme uses a spin mixing due to the spin–orbit interaction in the intermediate state. This scheme was first pointed out for the $\Omega = 1$ manifold consisting of $(1)^1\Pi$, $(2)^3\Sigma^+$ and $(1)^3\Pi$ [17] and demonstrated for RbCs [7] and for ^{40}K^{87}Rb [10]. In this scheme, the $(2)^3\Sigma^+$ state couples to the loosely bound molecules, whereas the $(1)^1\Pi$ state couples to the lowest rovibrational level.

In contrast, in the second scheme we can focus on a spin singlet state with large spatial overlaps of the wavefunctions. In fact, the experiment for Cs$_2$ at Innsbruck has been performed
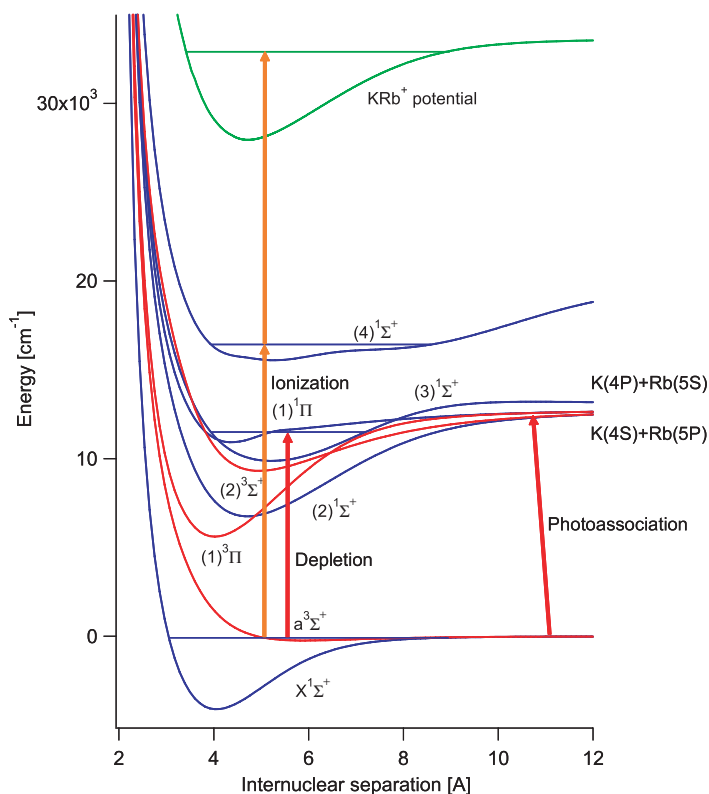
Figure 3. *Ab initio* potential energy curves of KRb [29]. Here only potentials related to our experiments are shown. Singlet and triplet potentials are indicated by blue and red curves, respectively.

based on this scheme [30]. For the case of KRb it was pointed out that the $(3)^1\Sigma^+$ state has favorable wavefunction overlaps both with loosely bound levels and the lowest level [31].

We are currently pursuing the second scheme using the $(3)^1\Sigma^+$ state. The $(3)^1\Sigma^+$ state has a purely singlet character; it can potentially couple with states dissociating to the K(4P) + Rb(5S) limit, but they are so far away from the $(3)^1\Sigma^+$ state that the spin–orbit coupling between them is negligible. The accurate potential energy curve of the $(3)^1\Sigma^+$ state has been found in a frequency range from $9778\,\mathrm{cm}^{-1}$ (potential minimum) to $10\,412\,\mathrm{cm}^{-1}$ by means of conventional spectroscopy of $^{39}\mathrm{K}^{85}\mathrm{Rb}$ molecules [32, 33]. Since the best candidate for the intermediate state for STIRAP lies between $11\,400$ and $11\,800\,\mathrm{cm}^{-1}$, the potential in this region has to be more precisely determined.

4.2. Experimental set-up

For spectroscopic studies, we prepared another experimental apparatus that can produce loosely bound molecules via photoassociation of laser-cooled $^{41}\mathrm{K}$ and $^{87}\mathrm{Rb}$ atoms following a similar experiment by the University of Connecticut group [31]. This set-up enables us to take a spectrum over a wide range of frequencies at a rate of $10\,\mathrm{Hz}$, which is much faster than taking a spectrum with Feshbach molecules. Figure 4 shows our experimental set-up for spectroscopy of loosely bound $^{41}\mathrm{K}^{87}\mathrm{Rb}$ molecules. First, 1×10^8 K atoms and 2×10^8 Rb atoms were cooled and trapped in a double-species MOT. Compressed MOT (C-MOT) was applied for both

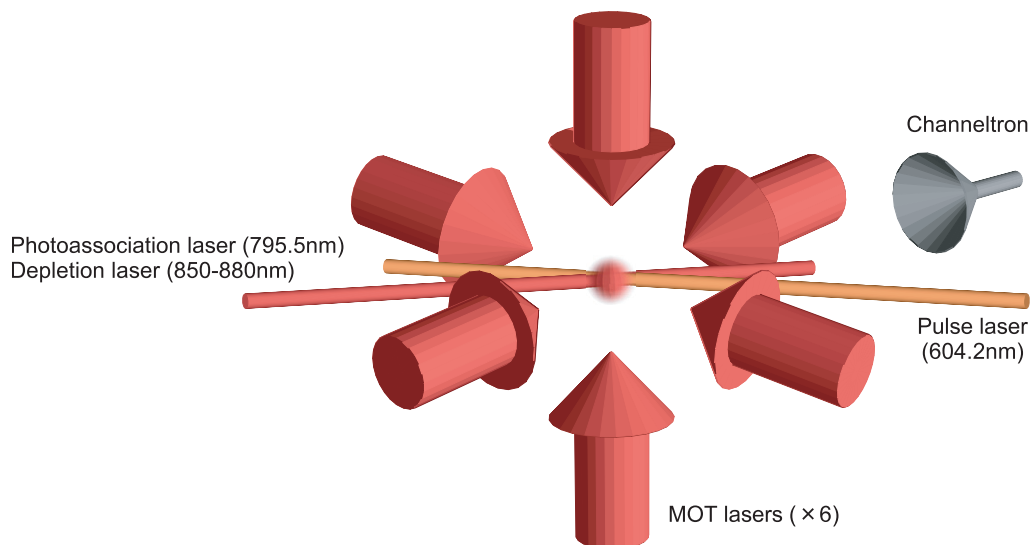**Figure 4.** Schematic diagram of the experimental set-up used for the depletion spectroscopy of ultracold ^{41}K^{87}Rb molecules. ^{41}K and ^{87}Rb atoms were cooled and trapped simultaneously in a MOT. The photoassociation laser was applied for 10 ms to form loosely bound X$^1\Sigma^+$ and a$^3\Sigma^+$ molecules, whereas the depletion laser was always turned on. Molecules in a specific vibrational level of the X$^1\Sigma^+$ state were ionized by an intense pulse laser and detected with a Channeltron ion detector.

clouds to cool and compress further to obtain number densities of 2×10^{11} cm^{-3} for K and 4×10^{11} cm^{-3} for Rb and temperatures of 400 μK for K and 100 μK for Rb. Both K and Rb atoms were prepared in their lower hyperfine states $F = 1$ during the C-MOT process. Then, a photoassociation laser with an intensity of 8.5 W cm^{-2} irradiated K and Rb atoms for 10 ms to form ground state molecules[8]. The frequency of the photoassociation laser was usually fixed at about 12 570.134 cm^{-1}, exciting the $J = 1$ level of the $\Omega = 0^+$ state. A tunable CW Ti:S laser with an intensity of 13 W cm^{-2} was simultaneously applied to molecules to deplete the population in a specific rovibrational level. Resultant molecules were detected with a Channeltron (Burle 4869) after they were ionized via resonance-enhanced multi-photon ionization induced by a pulsed dye laser with an intensity of 3×10^6 W cm^{-2}. Signals from the Channeltron were amplified with a homemade pre-amplifier [34] and sent to a high-speed digitizer (National Instruments PCI-5112) to count the number of molecules. Scanning the frequency of the Ti:S laser yielded a depletion spectrum that can resolve rotational structures of both ground and excited states.

The levels used for the two-photon ionization are indicated in figure 3. Molecules were first excited to the $v'' = 43$ level of the (4)$^1\Sigma^+$ state[9] and were then immediately excited to the ionization level. By selecting an appropriate wavelength for the ionizing pulse laser, we were able to monitor molecules in a specific vibrational level though the rotational structure could not be resolved due to a broad linewidth of the pulse laser (~ 0.1 cm^{-1}). We often used molecules in

---

[8] Typical $1/e^2$ beam diameter was 0.7 mm, which was nearly the same as the size of the MOT.

[9] The numbering given here has an uncertainty of a few quanta since the potential minimum of the (4)$^1\Sigma^+$ state has not yet been identified. This assignment of the vibrational number is based on the work on ^{39}K^{85}Rb by D Wang.
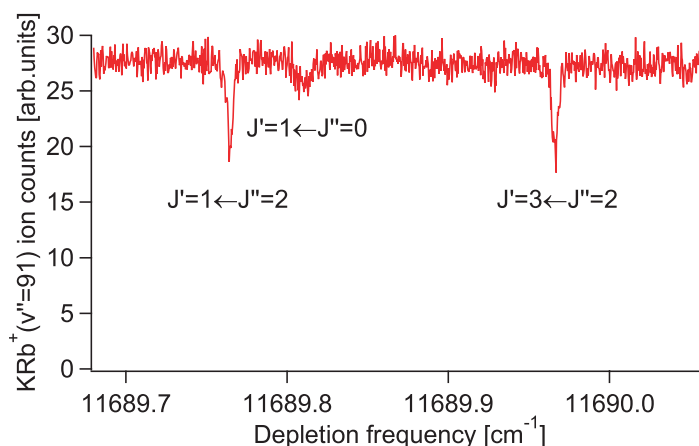
Figure 5. A depletion spectrum showing rotational structures of cold molecules. The spectrum was obtained by scanning the depletion laser while monitoring molecular ion counts. Each dip corresponds to a resonant excitation of molecules in the monitored level. Since we used the $J = 1$ rotational level for photoassociation, subsequent decays yielded ground state molecules in the $J'' = 0$ and 2 levels based on a selection rule $\Delta J = \pm 1$. The same selection rule also holds for an excitation from $X^1\Sigma^+$ to $(3)^1\Sigma^+$ states. Thus, three transitions were observed for a single upper vibrational level, namely, the $J' = 3 \leftarrow J'' = 2$, $J' = 1 \leftarrow J'' = 2$ and $J' = 1 \leftarrow J'' = 0$.

the $v'' = 91$, $J = 2$ level of the $X^1\Sigma^+$ state for spectroscopy of the excited state as they were the most abundant. The binding energy of this level was determined to be $-12.454(1)\,\mathrm{cm}^{-1}$ relative to the $F_{\mathrm{K}} = 1 + F_{\mathrm{Rb}} = 1$ threshold by comparing a depletion spectrum and a photoassociation spectrum for the same state.

4.3. Spectroscopy of the $(3)^1\Sigma^+$ state

Before taking a depletion spectrum, we performed a spectroscopy of the $(3)^1\Sigma^+$ states with a pulse laser as a rough guide in the frequency range from 11 340 to 11 740 cm^{-1}, where conventional spectroscopic studies have not been reported. Since the infrared photon does not have enough energy to ionize molecules via a two-photon transition, we simultaneously applied an additional 532 nm pulse laser derived from a pump laser for the pulsed dye laser. In this scheme, molecules were first excited by the infrared laser and immediately ionized by the green laser. To suppress a three-photon transition with the infrared laser and a two-photon transition with the green laser, we had to keep the intensity of the infrared and green lasers below 5×10^5 and $1 \times 10^5\,\mathrm{W\,cm}^{-2}$, respectively. Based on the obtained spectrum, we performed depletion spectroscopy for the $(3)^1\Sigma^+$ state. A typical spectrum for the $v'' = 48$ level of the $(3)^1\Sigma^+$ state is shown in figure 5. The narrow width of the spectrum ($\sim$100 MHz) enabled us to locate absolute energy levels of the excited state with much higher accuracy than using an *ab initio* potential, which typically has an error of the order of 10 cm^{-1} ($\sim$300 GHz).

To understand the observed spectrum, we need to consider the selection rule for rotational levels, i.e. $\Delta J = \pm 1$ [36]. Spontaneous decays from the photoassociation level of $J = 1$ yield the ground state molecules of $J = 0$ and 2. Molecules in $J = 0$ can only be excited to $J = 1$ of

the $(3)^1\Sigma^+$ state, whereas those in $J = 2$ can be excited to $J = 1$ and 3 of the $(3)^1\Sigma^+$ state. Thus, we obtain three transitions as shown in figure 5. From this spectrum, rotational constants of the $v'' = 91$ level of the $X^1\Sigma^+$ state and the $v'' = 48$ level of the $(3)^1\Sigma^+$ states were determined to be 0.00763(8) and 0.02017(1) cm^{-1}, respectively. The measured constant of the $X^1\Sigma^+$ state was in good agreement with that calculated from the experimentally determined accurate potential for the ground state [37] within the experimental error. We compared the measured constant of the $(3)^1\Sigma^+$ state with that obtained from the *ab initio* potential [29] and found that the *ab initio* potential gave a larger value by an amount of about 1%. This deviation has already been reported in [31] and should be attributed to the inaccuracy of the *ab initio* potential. We observed similar spectra for ten vibrational levels ($v'' = 41$–50) that were used to construct an accurate potential that can explain the measured energy levels and rotational constants [38]. Based on this potential, we conclude that the optimum intermediate state lies around the $v'' = 42$ level, which has Franck–Condon factors of about 10^{-2} with both the loosely bound level and the lowest rovibrational level [21].

5. Conclusion

In this paper, first we discussed key issues in the experimental design of quantum degenerate polar molecules. Then, first experimental results toward the realization of a Bose–Einstein condensate of ^{41}K^{87}Rb molecules were reported. A dual-species Bose–Einstein condensate of ^{41}K and ^{87}Rb was realized by evaporative cooling of rubidium atoms and sympathetic cooling of potassium atoms. Excited states of KRb molecules were studied using depletion spectroscopy and photoassociation. We plan to load a dual-species Bose–Einstein condensate of ^{41}K and ^{87}Rb into an optical lattice to form Feshbach molecules. A STIRAP transfer of loosely bound molecules will be studied using photoassociated ^{41}K^{87}Rb molecules. Finally, a STIRAP transfer will be applied to Feshbach molecules to produce a Bose–Einstein condensate of ^{41}K^{87}Rb molecules in the absolute ground state. The list of physics we would like to pursue with quantum degenerate polar molecules includes resonant features in collisions [39], the stability of the molecule [40] and the supersolid phase [2].

Acknowledgments

References

[1] Buchler H P *et al* 2007 *Phys. Rev. Lett.* **98** 060404
[2] Goral K, Santos L and Lewenstein M 2002 *Phys. Rev. Lett.* **88** 170406
[3] Micheli A, Brennen G K and Zoller P 2006 *Nat. Phys.* **2** 341
[4] Micheli A, Pupillo G and Buchler H P 2007 *Phys. Rev.* A **76** 043604
[5] Doyle J *et al* 2004 *Eur. Phys. J.* D **31** 149–64
[6] Bergmann K, Theuer H and Shore B W 1998 *Rev. Mod. Phys.* **70** 1003
[7] Sage J M, Sainis S, Bergeman T and DeMille D 2005 *Phys. Rev. Lett.* **94** 203001
[8] Lang F *et al* 2008 *Phys. Rev. Lett.* **101** 133005
[9] Danzl J G *et al* 2008 *Science* **321** 1062

[10] Ni K-K *et al* 2008 *Science* **322** 231
[11] Tagliever M *et al* 2008 *Phys. Rev. Lett.* **100** 010401
[12] Thalhammer G *et al* 2008 *Phys. Rev. Lett.* **100** 210402
[13] Simoni A *et al* 2008 *Phys. Rev.* A **77** 052705
[14] Wang H and Stwalley W C 1998 *J. Chem. Phys.* **108** 5767
[15] D'Incao J P and Esry B D 2008 *Phys. Rev. Lett.* **100** 163201
[16] Thalhammer G *et al* 2006 *Phys. Rev. Lett.* **96** 050402
[17] Bergeman T, Kerman A J, Sage J, Sainis S and DeMille D 2004 *Eur. Phys. J.* D **31** 179
[18] Pilch K *et al* 2008 arXiv:0812.3287
[19] Yatsenko L P, Romanenko V I, Shore B W and Bergmann K 2002 *Phys. Rev.* A **65** 043409
[20] Beuc R *et al* 2006 *J. Phys. B: At. Mol. Opt. Phys.* **39** S1191
[21] Naidon P 2008 private communication
[22] Koehler T, Goral K and Julienne P S 2006 *Rev. Mod. Phys.* **78** 1311
[23] Modugono G *et al* 2001 *Science* **294** 1320
[24] Kishimoto T *et al* 2008 arXiv:0812.4335
[25] Williamson R S and Walker T 1995 *J. Opt. Soc. Am.* B **12** 1393
[26] Prevedelli M *et al* 1999 *Phys. Rev.* A **59** 886
[27] Desruelle B *et al* 1999 *Phys. Rev.* A **60** R1759
[28] Hadzibabic Z *et al* 2003 *Phys. Rev. Lett.* **91** 160401
[29] Rousseau S, Allouche A R and Aubert-Frecon M 2000 *J. Mol. Spectrosc.* **203** 235
[30] Danzl J G *et al* 2008 arXiv:0811.2374
[31] Wang D *et al* 2007 *Phys. Rev.* A **75** 032511
[32] Amiot C, Verges J, d'Incan J and Effantin C 1999 *Chem. Phys. Lett.* **315** 55
[33] Amiot C, Verges J, d'Incan J and Effantin C 2000 *Chem. Phys. Lett.* **318** 289
[34] Flaxer E 2006 *Meas. Sci. Technol.* **17** N37
[35] Wang D 2007 *PhD Thesis* University of Connecticut
[36] Herzberg G 1950 *Molecular Spectra and Molecular Structure I. Spectra of Diatomic Molecules* (Princeton, NJ: Van Nostrand-Reinhold) (reprinted 1989 (Malabar: Krieger))
[37] Pashov A *et al* 2007 *Phys. Rev.* A **76** 022511
[38] Aikawa K *et al* to be published
[39] Ticknor C 2007 *Phys. Rev.* A **76** 052703
[40] Goral K and Santos L 2002 *Phys. Rev.* A **66** 023613